



ELSEVIER

Journal of Chromatography A, 744 (1996) 81–91

JOURNAL OF
CHROMATOGRAPHY A

Electrolytic modification of a buffer during a capillary electrophoresis run

Michael S. Bello

Dionex Corporation, 445 Lakeside Dr., Sunnyvale, CA 94088, USA

Abstract

The electrolyte composition and pH changes in the electrode reservoirs caused by the electric current in a capillary electrophoresis system are analyzed. Parameters determining the pH, electric conductivity and the ionic strength variations are the initial electrolyte composition, applied voltage, the capillary dimensions, volume of the reservoirs, and the electroosmotic flow. Equations for the pH and molarities of the electrolyte components as functions of time are derived. Experimentally measured pH shifts in the electrode reservoirs are in good agreement with the predicted values. The time interval after which the electrode buffer needs to be replenished is determined as a function of the electric field strength, mobilities of the buffer ions, capillary cross-section and volume of the buffer in the reservoir.

Keywords: Buffer composition; pH changes

1. Introduction

The properties of a buffer in the electrode reservoirs change during the run because of electrochemical reactions at the electrodes. In capillary electrophoresis (CE), water hydrolysis frequently takes place at the electrodes. Therefore, the electric current leads to an accumulation of cations at the cathode reservoir and to their depletion at the anode. The anions accumulate at the anode reservoir and deplete at the cathode. This redistribution of ions between the anode and cathode electrolytes by the electric current is called electrolytic modification of the buffer, which results in the buffer pH increasing at the cathode and decreasing at the anode. The electrical conductivity and ionic strength of the buffer also change, affecting reproducibility of consecutive separations performed with the same buffer. Replenishment of the buffer reservoirs is generally recommended after a series of runs. An improved

migration time reproducibility was obtained by replenishing the buffer between runs [1].

The pH in the buffer reservoirs influences CE separation by (i) affecting the migration time through variation of the electroosmotic (EO) flow, and (ii) directly changing mobilities of the analytes sensitive to the pH. The effect of the solution pH on the EO flow in the capillary is well understood. The solution pH controls the degree of ionization of the surface silanols having pK between 6 and 7 [2]. Several authors [3–9] have shown that the EO mobility exhibits a characteristic sigmoidal dependence on pH, with the steepest slope located at neutral pH. Therefore, variations of the buffer pH, especially in this region, are potentially dangerous to the reproducibility of the EO flow. The direct effect of the solution pH in the electrode reservoirs on the migration time of trypsinogen has been systematically studied by Strege and Lagu [9], who excluded EO flow effects by using a coated capillary with virtually

negligible EO mobility. The migration time of trypsinogen was measured [9] for nine consecutive runs from the same vials with sodium phosphate and sodium acetate buffers, both at pH=4.3. In the phosphate buffer, the protein migration time decreased from run-to-run, changing approximately 25% between the first and ninth runs. The pH in the electrode reservoirs was found to be 3.41 and 5.45 in the anode and cathode reservoirs, respectively. Replenishing the electrode buffer after every run resulted in excellent migration time reproducibility. The acetate buffer showed an almost negligible change of pH values in the electrode reservoirs after nine runs and a very gentle slope of the migration time dependence on the run number. A gradual deterioration of resolution from run to run and the pH change of the buffer has been recently reported [10].

Electrokinetic injection is another instance where electrolytic modification affects CE. In CE, it is common to prepare a sample dissolved in water, in which case the buffering capacity of the sample is very low. When an electrokinetic injection is applied to such a sample, even a short injection time is sufficient to alter the pH and/or electric conductivity, resulting in poor reproducibility of the injection [1,11].

Strege and Lagu [9] provided a valuable investigation of the effect of the buffer electrolytic modification on migration time and showed the importance of using a buffer with good buffering capacity (acetate versus phosphate at pH=4.3). However, it is desirable to determine the degree to which the buffer composition is changed after a series of runs, and how often the buffer should be replenished for an arbitrary chosen buffer and CE system. It may be assumed that changes of pH values in the electrode reservoirs depend on the buffering capacity of the buffer, duration of the run, applied voltage, volume of the electrode reservoirs, and other parameters.

This paper studies pH changes in the electrode reservoirs, both theoretically and experimentally. A simplified theory describes the pH and concentration changes in the electrode vials. Experimental measurements of the pH and electric conductivity in the vials after the voltage has been applied are compared with the theoretical predictions. Time dependence of

the pH in the capillary is derived from the experimental data [9] and compared with a theoretical curve. The rate of the pH change in the vial is determined as a function of the intensity of the electric field, the capillary cross-section area, and the buffer composition. Frequency of the buffer replenishment is also discussed.

2. Theoretical

Fig. 1 shows a simple CE system consisting of two electrodes, two electrode reservoirs, a capillary, and a power supply. The reservoirs and capillary are filled with an aqueous electrolyte solution. The anode and cathode reservoirs contain, respectively, volume V_A^0 and volume V_C^0 of the solution. The solution is composed of a weak acid [A_W], a strong acid [A_S], and a strong base [B]. The power supply maintains a constant potential difference U between the two electrodes.

The voltage applied to the electrodes generates an electric current and transports anions toward the anode and cations toward the cathode. The anions enter the anode reservoir and the cations leave it. The excess negative charge is compensated by an increasing concentration of protons generated at the electrode; thus, pH of the solutions decreases at the anode. The opposite process occurs at the cathode: the excess positive charge brought by the electric current is neutralized by hydroxyl ions, resulting in an elevation of the solution pH.

The theoretical considerations below are aimed at relating the rates at which the solution pH changes with the system parameters.

To simplify the analysis, the following assumptions are made: (1) The solution is electrically neutral; (2) the only electrode process in the system is the water hydrolysis; (3) ion mobilities and the dissociation constant of the weak acid are equal to those at infinite dilution; (4) the influence of pH and conductivity changes on the electric current is negligible and the electric current is constant; (5) the EO flow is constant during the run; and (6) molecular diffusion is negligible.

To estimate pH change in the buffer reservoirs one must evaluate the cation and anion fluxes in and out of the electrode reservoirs.

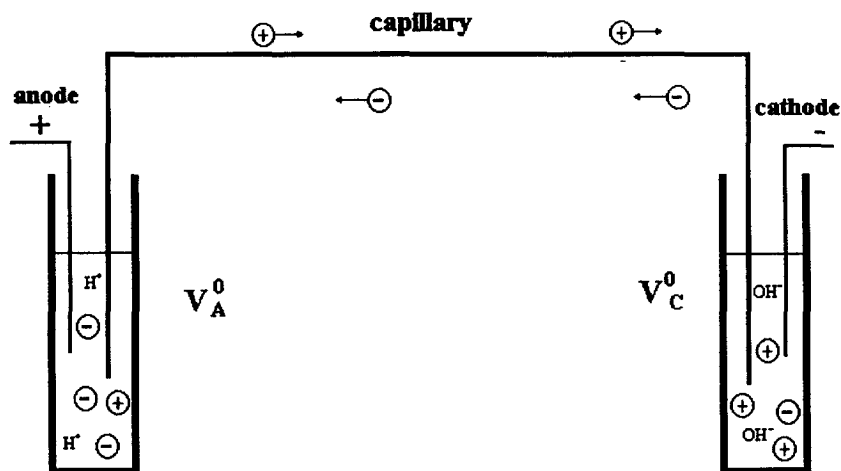


Fig. 1. Sketch of the analyzed system composed of two reservoirs and two electrodes connected by the capillary. The reservoirs and the capillary are filled with the solution. Electric current leads to an increase of the anion concentration and a decrease of the cation concentration in the anode reservoir. The excess charge brought by the electric current is neutralized by increased concentrations of protons and hydroxyl ions at the anode and cathode, respectively.

2.1. Anode reservoir

Mole fluxes of the weak acid, strong acid, and base out of the reservoir are given by

$$J_w = [A_w]S_c(\mu_w EK/(K + [H]) + U_{OS}) \quad (1a)$$

$$J_s = [A_s]S_c(\mu_s E + U_{OS}) \quad (1b)$$

$$J_B = [B]S_c(\mu_B E + U_{OS}) \quad (1c)$$

where J_w , J_s , J_B are the molar fluxes out of the anode reservoir of the weak acid, strong acid anion and strong base cation, respectively; $[A_w]$, $[A_s]$ and $[B]$ are their respective molarities in the reservoir; μ_w , μ_s , μ_B are the respective ion mobilities in the fully ionized state; E is the intensity of the electric field; K is the dissociation constant of the weak acid; $[H]$ is the molarity of the protons; U_{OS} is the EO velocity; and S_c is the capillary cross-section area. The mobilities of the anions are assumed to be negative.

A time derivative of the molarity of any substance in the reservoir can be found as follows:

$$\begin{aligned} d[C]/dt &\equiv d(M/V_A)/dt \\ &\equiv (dM/dt)/V_A - M/V_A^2 dV_A/dt \\ &\equiv (dM/dt)/V_A - ([C]/V_A)dV_A/dt, \end{aligned}$$

$$dM/dt = -J \quad (2)$$

where $[C]$ is the molarity of a substance in the anode reservoir, t is the time, M is the number of moles of a substance in the anode reservoir, V_A is the volume of liquid in the anode reservoir, and J is the molar flux of a substance out of the reservoir.

The rate at which the solution volume in the anode reservoir decreases is determined by the EO flow and is given by

$$dV_A/dt = -S_c U_{OS} \quad (3)$$

Substitution of Eqs. 1 and 3 into Eq. 2 for all three buffer components results in the following equations describing the evolution of molarities of the buffer components:

$$d[A_w]/dt = -[A_w](S_c E/V_A)\mu_w K/(K + [H]) \quad (4a)$$

$$d[A_s]/dt = -[A_s](S_c E/V_A)\mu_s \quad (4b)$$

$$d[B]/dt = -[B](S_c E/V_A)\mu_B \quad (4c)$$

Initial conditions to Eqs. 4 are

$$\begin{aligned} [A_w]_{t=0} &= [A_w]^0, & [A_s]_{t=0} &= [A_s]^0, \\ [B]_{t=0} &= [B]^0 \end{aligned} \quad (5)$$

where $[A_w]^0$, $[A_s]^0$ and $[B]^0$ are the concentrations

of the weak acid, strong acid anion and strong base cation in the reservoir before the voltage has been applied.

Eqs. 4a, b and c contain $[H]$ and V_A , which also depend on time. The volume of the buffer in the anode reservoir is easily found from Eq. 3.

$$V_A = V_A^0 - SU_{OS}t \quad (6)$$

where V_A^0 is the initial volume of the buffer in the anode reservoir.

The molarity of protons can be found from the electroneutrality equation

$$[A_w](K/(K + [H])) + [A_s] + K/[H] = [H] + [B] \quad (7)$$

where K_w is the water ionization constant, $K_w \approx 10^{-14} \text{ mol}^2/\text{l}^2$.

The three first order ordinary differential Eqs. 4a, b and c with three initial conditions Eq. 5, and two algebraic equations Eqs. 6 and 7 contain five unknowns and can be solved numerically. The result of this solution is the molarities of all species as functions of time. Formulas for the solution pH, ionic strength, and specific conductivity can be found in Appendix A.

Instead of solving Eqs. 4–7, one can do some additional treatment leading to approximate but explicit relationships between the pH rate and characteristics of the process.

By taking derivatives of both sides of Eq. 7 with respect to time one obtains

$$\begin{aligned} (d[A_w]/dt)K/(K + [H]) - [A_w]K/(K + [H])^2 d[H]/dt - K_w/[H]^2 d[H]/dt + d[A_s]/dt \\ = d[H]/dt + d[B]/dt \end{aligned} \quad (8)$$

Substitution of Eq. 4 into Eq. 8 results in

$$\begin{aligned} d[H]/dt(1 + [A_w]K/(K + [H])^2 + K_w/[H]^2) \\ = (SE/V_A)(\mu_B[B] - [A_w]\mu_w K^2/(K + [H])^2 \\ - [A_s]\mu_s) \end{aligned} \quad (9)$$

Eq. 8 can be rewritten in an equivalent form

$$\begin{aligned} dpH/dt = -(1/\ln 10)(SE/V_A)([B]\mu_B \\ - [A_w]\mu_w K^2/(K + [H])^2 \\ - [A_s]\mu_s)/([H] + [A_w]K/[H])/(K + [H])^2 \end{aligned}$$

$$+ K_w/[H]) \quad (10)$$

where $pH = -\log [H]$ and $\ln 10$ is the natural logarithm of 10, $\ln 10 \approx 2.3$.

The initial conditions of Eq. 9 or Eq. 10 are the initial H or pH values of the buffer.

Several conclusions can be deduced from Eqs. 9 and 10. It is seen from Eq. 10 that the rate of the pH decrease is proportional to the electric field strength and the capillary cross-section area, and inversely proportional to the volume of the solution. Therefore, the smaller the volume V_A , the larger the cross-section area, and the higher the electric field strength, the faster the pH decreases in the anode reservoir.

Eq. 10 can be further transformed by defining the solution buffering capacity, which is the number of moles of a strong acid or base added to the solution that would change pH by 1 unit. The following expression for the buffering capacity can be obtained by differentiating Eq. 7 over pH

$$\begin{aligned} \beta &\equiv d([B] - [A_s])/dpH, \\ \beta &= \ln 10([H] + [A_w][H]K/(K + [H])^2 + K_w/[H]) \end{aligned} \quad (11)$$

where β is the buffering capacity.

By taking into account Eq. 11, Eq. 10 can be rewritten as

$$\begin{aligned} dpH/dt = -(SE/V_A)([B]\mu_B - [A_w]\mu_w K^2/ \\ (K + [H])^2 + [A_s]\mu_s)/\beta \end{aligned} \quad (12)$$

This equation shows that the higher the buffering capacity of the solution, the lower the rate of the pH decrease. The theory presented here can be easily extended for a general case of a solution composed of an arbitrary number of anions and cations. Additional equations and terms corresponding to additional species should be included in a set of Eqs. 4 and 7, respectively. Derivation of a multicomponent analog to Eqs. 11 and 12 is straightforward and is omitted in this paper.

2.1.1. Buffer at $pH = pK$

Let us consider a case in which the buffering capacity has its maximum value and no strong acid is present in the solution. Then the solution pH is equal to the pK of the weak acid, and the molarity of the

strong base cation is equal to half the molarity of the weak acid.

$$[H] = K, \quad [B] = [A_w]/2, \quad [A_s] = 0 \quad (13)$$

Assume also that the molarity of the weak acid $[A_w]$ is much greater than its dissociation constant K ($[A_w] \gg K$) and the ratio K_w/K ($[A_w] \gg K_w/K$). These assumptions mean that concentrations of protons and hydroxyl ions are negligible compared to the concentration of the weak acid. Under this condition, the first and third terms in Eq. 11 for buffering capacity can be omitted and Eq. 11 simplifies to

$$\beta = [A_w] \ln 10/4 \quad (14)$$

For relatively small pH deviations from the pK one obtains from Eqs. 12–14

$$dpH/dt = -(SE/V_A)(\mu_w + 2\mu_B)/\ln 10 \quad (15)$$

The solution to Eq. 15 is straightforward and is given by

$$pH = pK + E(\mu_w + 2\mu_B) \log(1 - SU_{OS}t/V_A^0)/U_{OS} \quad (16a)$$

For most practical cases, the relative volume of the buffer removed by the EO flow is much less than 1, $SU_{OS}t/V_A^0 < 1$. Under this condition, Eq. 16a further simplifies to

$$pH = pK - t(SE/V_A^0)(\mu_w + 2\mu_B)/\ln 10 \quad (16b)$$

However, the effect of the EO flow is not negligible when small electrode reservoirs are used and the EO flow is strong enough.

Two important conclusions can be drawn from Eq. 15 for the buffer containing no strong acid and adjusted to its maximum buffering capacity ($pH = pK$).

1. The pH in the anode reservoir decreases with a rate independent of the buffer molarity.
2. The rate of pH change is higher for the buffer containing high mobility ions.

An intuitive explanation of the pH change independence of the buffer molarity is that both the buffering capacity and electric conductivity are

proportional (as a zero order approximation) to the buffer molarity. Thus, the higher the buffering capacity, the higher the electric current and, hence, more of a charge must be neutralized.

Eq. 16b also makes it easy to estimate the frequency of buffer replenishment in a CE system. Assume that the pH and ionic strength decrease of the anode buffer by ϵ leads to an undesirable shift of the migration time. It follows from Eq. 16b (or Eq. 15) that the time Δt it takes to decrease the pH by ϵ , is given by

$$\Delta t = \epsilon \ln 10 V_A / [SE(\mu_w + 2\mu_B)] \quad (17)$$

Suppose that a capillary has an inner diameter of 75 μm , the intensity of the electric field is $E = 5 \cdot 10^4$ V/m, the vial volume is $V_A = 10^{-6}$ m³, $\mu_w = -4.1 \cdot 10^{-8}$ m²/(V s) (boric acid anion), $\mu_B = 5.3 \cdot 10^{-8}$ m²/(V s) (sodium cation), and the pH change is $\epsilon = 0.05$. Substituting these values into Eq. 17 gives

$$\Delta t \cong 1 \text{ h}$$

Therefore, the running buffer should be changed every hour. It is now evident that for a run taking 5 min, the buffer should be changed every twelfth injection, and for a run taking 20 min it should be changed every third injection. Under the same conditions, but for a 50 μm I.D. capillary instead of 75 μm , the replenishment time is $(75/50)^2 = 2.25$ h.

2.1.2. Strong electrolyte

Another case that can easily be analyzed by the presented theory is the solution of a strong electrolyte. If one neglects the contribution of the protons and/or hydroxyl ions to the electric conductivity, Eq. 9 simplifies to

$$d[H]/dt = I/(FV_A) \quad (18)$$

where F is the Faraday constant.

By using the definition of pH and integrating Eq. 18 one obtains

$$pH = -\log(K_w^{1/2} + 10^{-3}I/(FV_A)t) \quad (19)$$

The factor 10^{-3} appears in Eq. 19 because the molarity of $[H]$ should be measured in mol/l rather than in mol/m³.

It follows from Eq. 18 that for an electric current of 10 μA and a volume of solution in the anode

reservoir $V_A=1$ ml, the pH of the solution will become pH=6 after 10 s, pH=5.2 after 1 min, and pH=3.74 after 30 min since the voltage has been applied to the system.

2.2. Cathode reservoir

Electrolytic modification of the cathode buffer can be analyzed analogously to the above anode case. Differences between equations describing the electrolytic modification in the anode and reservoir are (i) the right hand sides of Eqs. 1, 3 and 4 change signs, and (ii) the hydroxyl molarity $[OH]$ should be taken as an unknown variable instead of $[H]$.

The volume of the buffer in the cathode reservoir is given by

$$V_C = V_C^0 + SU_{O_3}t \quad (20)$$

where V_C is the volume of the buffer in the cathode reservoir at time t , and V_C^0 is the initial volume.

The volume of liquid V_C in the cathode reservoir increases due to the EO flow pumping the fluid at the same rate it decreases in the anode reservoir. Eq. A3 gives the evolution of the hydroxyl molarity in the cathode reservoir (see Appendix A). Derivation of all formulas describing modification of the cathode buffer is omitted for the sake of brevity.

2.2.1. Buffer at $pH=pK$

The analog to Eq. 16b describing the pH evolution in the cathode reservoir in the case of a buffer at $pH=pK$ is given by

$$pH = pK + t(SE/V_C^0)(\mu_w + 2\mu_b)/\ln 10 \quad (21)$$

where V_C^0 is the volume of the buffer in the cathode reservoir.

One can see from Eq. 21 that pH in the cathode reservoir increases linearly with time. The rate of the pH increase is the same as the pH decrease in the anode reservoir.

2.2.2. Strong electrolyte

The hydroxyl molarity in the cathode reservoir is governed by

$$d[OH]/dt = I/(FV_A) \quad (22)$$

The approximate equation for pH in this case is

$$pH = -\log(K_w) + \log(K_w^{1/2} + 10^{-3} I/(FV_A)t) \quad (23)$$

These equations predict that pH growth in the cathode reservoir will occur at the same rate as the pH decrease in the anode reservoir.

3. Experimental

Because of the assumptions made, the theory presented above needs an experimental verification. Additionally, approximate solutions 16b, 19, 22 and 23 should be compared with the numerical solution to Eqs. 4–6 and 9 and their cathode analogs.

To test the theory, high voltage was applied to a capillary for a long period. The buffer vials were weighed before and after each run and the pH in the vials was measured. A weight difference was attributed to the EO flow and was used for estimating the average EO mobility.

3.1. Materials and methods

Three types of electrolyte solutions were used: 10 mM KCl standard solution $\sigma=1.413$ as a strong electrolyte, 2 mM sodium tetraborate decahydrate as a buffer at $pH=pK$, and a mixture composed of 2 mM sodium tetraborate decahydrate and 4 mM NaCl. Sodium chloride and potassium chloride were from Fisher Chemical, Fair Lawn, NJ, USA, and sodium borate decahydrate was from Sigma, St. Louis, MO, USA. Fused-silica capillaries (Polymicro Technologies, Phoenix, AZ, USA) were 50 cm \times 75 μ m I.D. One of the capillaries was treated with a polymer solution and exhibited slightly lower EO mobility than the other. The pH was measured by a Phi-40 pH meter equipped with a microelectrode (Beckman Instruments, Fullerton, CA, USA). All runs were performed on a Dionex (Sunnyvale, CA, USA) prototype CE instrument. The volume of the electrolyte in the electrode reservoirs was either 3.5 or 1 ml. Electric field strength was $5 \cdot 10^4$ V/m. The duration of the run was 180 min with 3.5 ml of the electrolyte and 120 min with 1 ml. The numerical solution to Eqs. 4–6 and 9 was obtained by using the Euler method and gave an adequate precision. Computer programs were written and implemented on a 486/DX2 PC.

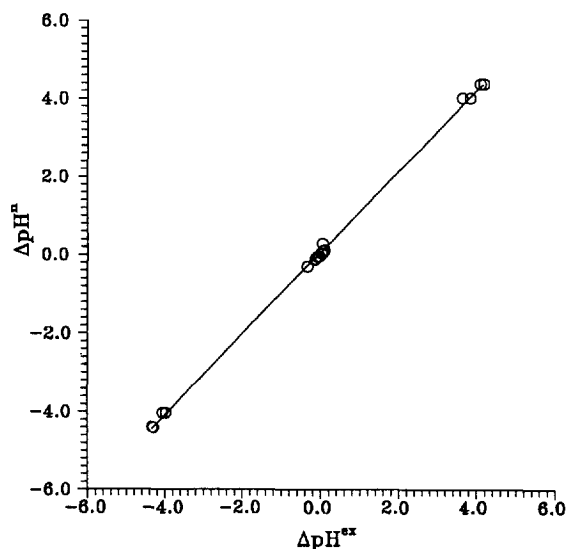


Fig. 2. Theoretically calculated shift of pH in the cathode and anode reservoirs versus experimentally measured shifts. Positive and negative values correspond to the cathode and anode reservoirs, respectively. 50 cm \times 75 μ m I.D. capillary, 25 kV.

4. Results and discussion

Fig. 2. shows the correlation between the pH change calculated numerically and measured experimentally. The agreement between the theoretical and experimental values is good in the wide range of pH values. More details are presented in Table 1.

Some observations can be made about the results

presented in the Table: (1) The numerical solution and approximate formulas give almost indistinguishable results; therefore, the approximate equations can be used for the cases of the buffer at $\text{pH} = \text{pK}$ and strong electrolyte. (2) Theoretical predictions for the anode pH shift are in better agreement with experimental values than those for the cathode pH shift. The maximum error corresponds to the run made with a 1 ml volume. This can be explained by the presence of the EO flow, which transports liquid with the low pH from the anode reservoir to the cathode reservoir, thus lowering the pH in the cathode reservoir. Therefore, a comparison of the experimental and theoretical results confirms that the theory of the electrolyte modification is valid and can be applied for predicting pH changes in the electrode vials.

An additional test to this theory can be done by comparing its predictions with the data reported by Strege and Lagu [9]. Although they did not measure pH in the anode vial as a function of time, Fig. 3 in Ref. [9] presents a graph for the trypsinogen migration time as a function of run number (each run took 60 min). Fig. 7 in Ref. [9] shows the trypsinogen migration time as a function of the buffer pH. It is possible to combine the data shown in both graphs to obtain the buffer pH as a function of time and compare it with the numerical solution to Eqs. 4–6 and 9.

Three experimental points of the trypsinogen

Table 1
Comparison of experimental and calculated pH shifts in the electrode reservoirs

Number	Volume (ml)	Electrolyte composition	Initial pH	$\Delta\text{pH}_A^{\text{ex}}$	$\Delta\text{pH}_A^{\text{n}}$	$\Delta\text{pH}_A^{\text{a}}$	$\Delta\text{pH}_C^{\text{ex}}$	$\Delta\text{pH}_C^{\text{n}}$	$\Delta\text{pH}_C^{\text{a}}$	$\mu_{\text{OS}} \cdot 10^{-8} \text{ m}^2/\text{V/s}$
1	3.5	2 mM $\text{Na}_2\text{B}_4\text{O}_7$	9.23	-0.05	-0.04	-0.04	0.03	0.04	0.04	9.64
2	3.5	2 mM $\text{Na}_2\text{B}_4\text{O}_7$	9.23	-0.08	-0.04	-0.04	0.01	0.04	0.04	9.8
3	3.5	2 mM $\text{Na}_2\text{B}_4\text{O}_7$	9.27	-0.04	-0.04	-0.04	0.03	0.04	0.04	9.07
4	1	2 mM $\text{Na}_2\text{B}_4\text{O}_7$	9.23	-0.14	-0.10	-0.10	0.07	0.10	0.10	9.87
5	1	2 mM $\text{Na}_2\text{B}_4\text{O}_7$	9.27	-0.13	-0.1	-0.10	0.06	0.10	0.10	8.96
6	3.5	2 mM $\text{Na}_2\text{B}_4\text{O}_7$ + 4 mM NaCl	9.16	-0.14	-0.12	-0.12	0.09	0.12		8.25
7	1	2 mM $\text{Na}_2\text{B}_4\text{O}_7$ + 4 mM NaCl	9.16	-0.33	-0.3	-0.3	0.04	0.29		7.87
8	3.5	10 mM KCl	7	-3.98	-4.03	-4.03	3.83	4.02	4.02	4.12
9	3.5	10 mM KCl	7	-4.06	-4.03	-4.03	3.63	4.02	4.02	5.20
10	1	10 mM KCl	7	-4.33	-4.40	-4.39	4.18	4.38	4.39	3.08
11	1	10 mM KCl	7	-4.3	-4.41	-4.39	4.09	4.38	4.39	3.93

$\Delta\text{pH}_A^{\text{ex}}$, $\Delta\text{pH}_A^{\text{n}}$ and $\Delta\text{pH}_A^{\text{a}}$ are, respectively, experimentally measured, numerically calculated, and calculated by using approximate formulas, pH shifts in the anode vial; $\Delta\text{pH}_C^{\text{ex}}$, $\Delta\text{pH}_C^{\text{n}}$ and $\Delta\text{pH}_C^{\text{a}}$ are, respectively, experimentally measured, numerically calculated, and calculated by using approximate formulas, pH shifts in the cathode vial; μ_{OS} is the average EO mobility.

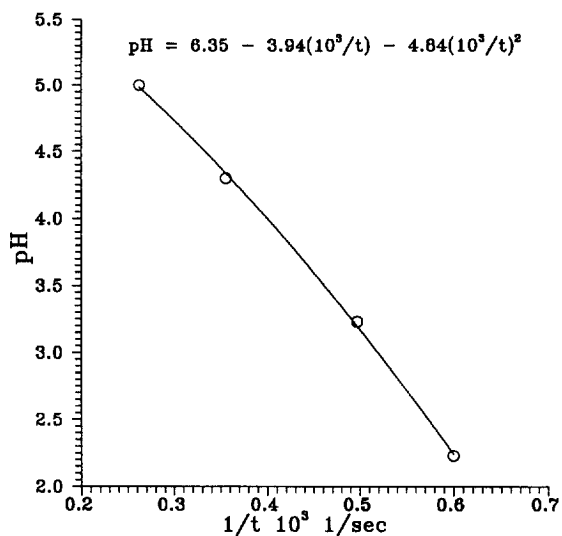


Fig. 3. Buffer pH versus migration time. Data points taken from Strege and Lagu [9].

migration time (1664, 2014, and 3813 s corresponding to pH 2.23, 3.23 and 5.0, respectively) were taken from Ref. [9] (Fig. 7). The migration time of 2835 s corresponding to pH=4.3 was taken from Ref. [9] (Fig. 3). The abscissa in Fig. 3 is the scaled reciprocal migration time that is proportional to the electrophoretic mobility of the analyte. The ordinate is the buffer pH. The equation providing the best fit to the experimental points is shown in Fig. 3. It was further used to transform migration times from Fig. 3 in Ref. [9] into the pH values.

Fig. 4 shows the buffer pH values as a function of time extracted from Ref. [9] and calculated by using Eqs. 4–6 and 9. The calculated and experimental curves show a similar trend for both phosphate and acetate buffers.

Discrepancies between the experimental data and theoretical predictions in Fig. 4 are attributed to: (i) experimental errors, (ii) errors introduced when the experimental points were taken from the graphs, (iii) errors of the best-fit equation, and (iv) uncertainty of the time to which the experimental points should be assigned. Given the approximate character of the theory presented and the sources of errors listed above, the agreement between the experimental results [9] and theoretical curves in Fig. 4 should be considered good.

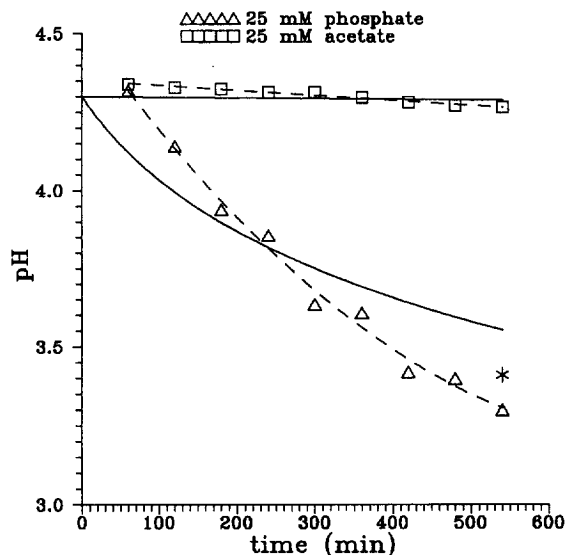


Fig. 4. Experimental and theoretical pH dependencies on time for 25 mM sodium phosphate and 25 mM sodium acetate. 97 cm \times 50 μ m I.D. capillary, 25 kV. Experimental data shown by triangles and squares are extracted from Strege and Lagu [9]. Solid lines are theoretical curves calculated by using Eqs. 4–6 and 9 assuming that the volumes of the reservoirs are 4 ml. The asterisk indicates the pH measured in the anode reservoir after the ninth run [9].

Fig. 5 shows plots of pH of 2 mM sodium tetraborate in the anode reservoir as functions of time for different volumes of the solution calculated by using Eq. 16b. The steepest pH decrease occurs for the smallest volume of 0.5 ml. Here, either the buffer solution should be replenished frequently, or 50 or 25 μ m capillaries should be used instead of the 75 μ m I.D. capillary. The effect of electrolytic modification on the pH value is almost negligible when the reservoir contains 10 ml of the solution.

Plots of pH in the anode reservoir as functions of time for 2 mM sodium tetraborate, a solution containing 2 mM sodium tetraborate and 4 mM NaCl, and a solution containing 2 mM sodium tetraborate and 8 mM NaCl are shown in Fig. 6. In all cases pH decreases linearly with time. The steepest decrease corresponds to the solution with the highest concentration of the salt added to the buffer.

Fig. 7 illustrates the evolution of the electric conductivity in the anode reservoir for the same solutions and conditions as in Fig. 6. Electric conductivity and ionic strength were calculated accord-

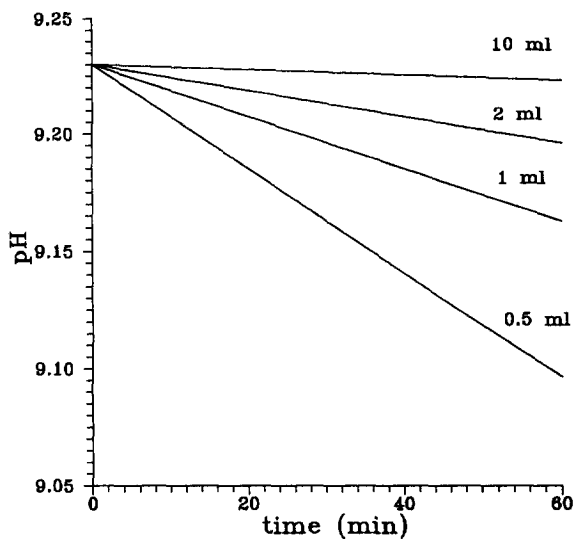


Fig. 5. Simulation of the pH course in anode reservoirs of different volumes. 2 mM sodium tetraborate, 50 cm \times 75 μ m I.D. capillary, 25 kV.

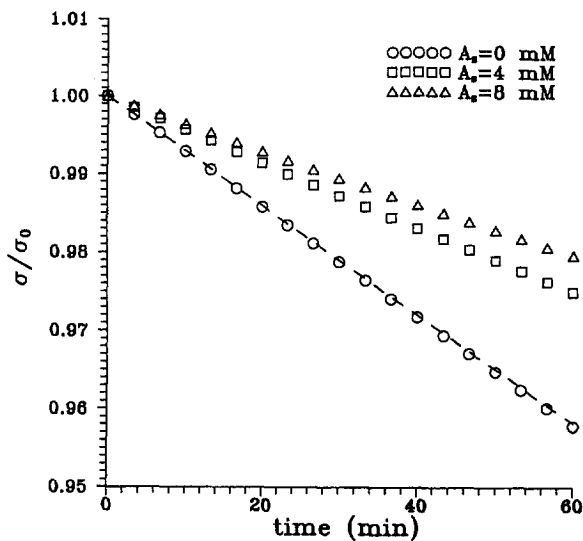


Fig. 7. Simulation of the electric conductivity course in the anode reservoir for the same parameters as Fig. 6.

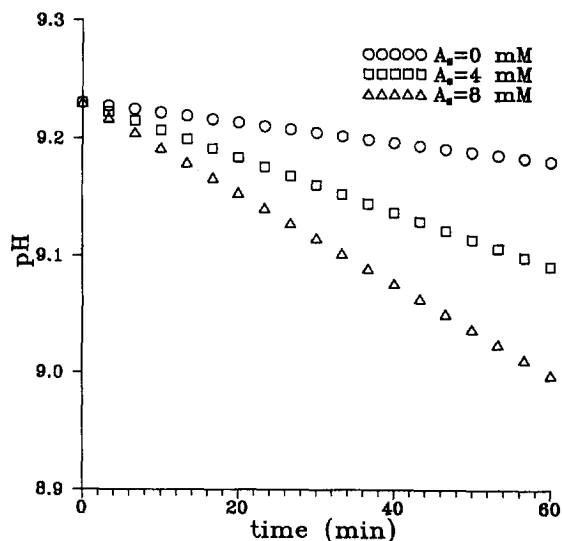


Fig. 6. Simulation of the pH course in the anode reservoir for 2 mM sodium tetraborate ($A_s=0$, $A_w=8$ mM, $B=4$ mM), a solution containing 2 mM sodium tetraborate and 4 mM NaCl tetraborate ($A_s=4$ mM, $A_w=8$ mM, $B=8$ mM), and a solution containing 2 mM sodium tetraborate and 8 mM NaCl ($A_s=8$ mM, $A_w=8$ mM, $B=12$ mM). 50 cm \times 75 μ m I.D. capillary, 25 kV.

ing to Eqs. A1 and A2 in Appendix A. The most significant change in the electric conductivity is found for the pure sodium tetraborate buffer, in contrast to the previous case of the pH variation. The electric conductivity decreases as a result of the pH decrease in the anode reservoir. The most stable electric conductivity is found for the buffer with the highest concentration of NaCl. In practice, a decreased electric conductivity caused by the electrolytic modification reveals itself in a decreasing electric current in the capillary. However, a complex buffer containing additional salt may show a stable current while having significant variation in pH. The dashed line in Fig. 7 shows a decrease in the ionic strength of the buffer in the anode vial. The ionic strength change also contributes to the variations of the EO flow in the capillary.

Fig. 8 shows the pH time dependence in the anode reservoir for 10 mM solutions of KCl with additions of buffering compound (potassium borate). In pure KCl the pH drops almost immediately to 5 and then decreases further. This curve is described by Eq. 19. Adding a small amount of the buffering compound (0.1 mM potassium borate) delays the pH drop. A further addition of the buffer stabilizes the solution pH for a relatively long time, although when the buffering capacity is exhausted, a steep transition

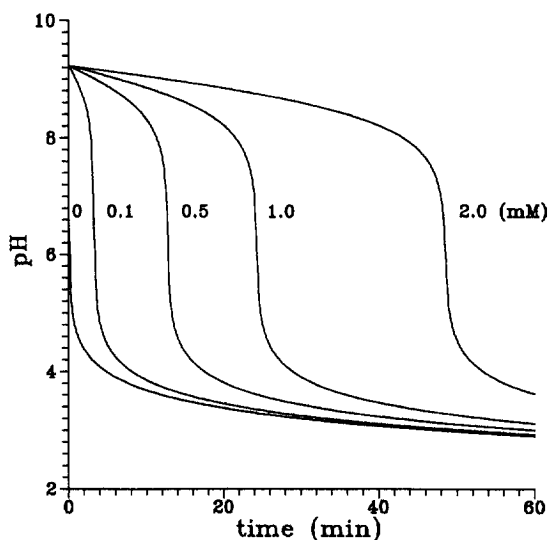


Fig. 8. Simulation of the pH course in the anode reservoir for 10 mM solutions of KCl with additions of buffering compound (potassium borate). Curve marked with 0 corresponds to $A_s=10$ mM, $A_w=0$ mM, $B=10$ mM, $\text{pH}=7$. Other curves were calculated for $A_s=10$ mM in all simulations and $A_w=0.1$ mM, $B=10.05$ mM; $A_w=0.5$ mM, $B=10.25$ mM; $A_w=1$ mM, $B=10.5$ mM; $A_w=2$ mM, $B=11$ mM, $\text{pH}=\text{p}K=9.23$.

to a low pH occurs. This transition corresponds to the buffer titration with an acid.

5. Conclusions

The theory and its experimental verification presented here make it possible to predict pH change in the electrode reservoirs for a given composition of the solution, reservoir volume, electric field strength, EO flow, and capillary I.D. The smaller the volume of the vial, and the higher the electric field strength and the larger the capillary cross-section area, the more significantly the pH of the buffer changes during a run. In a buffer having a maximum buffering capacity ($\text{pH}=\text{p}K$), the pH change is independent of the buffer molarity and, therefore, an increase of the buffer molarity does not stabilize the pH in the electrode reservoirs. The value of the pH change can be estimated by using Eq. 16b for the anode reservoir and Eq. 21 for the cathode reservoir. Eq. 17 enables one to estimate how often the electrode reservoirs should be replenished. To do this one

decides the pH change acceptable for a planned series of runs and calculates the time it takes to obtain this pH change. The example presented in this paper shows a need to replenish the buffer after the voltage has been applied for 1 h.

6. List of Symbols

6.1. Latin

[A]	molarity of the acid
[B]	molarity of the base
[C]	molarity of any component
E	intensity of the electric field
F	Faraday constant
[H]	molarity of protons
I	electric current
i	ionic strength
J	mass flux
K	ionization constant of the weak acid
K_w	ionization constant of water
M	number of moles of any component in the reservoir
[OH]	molarity of the hydroxyl ion
S	cross-section area of the capillary
U_{OS}	electroosmotic velocity
V	volume of the solution in the reservoir
t	time

6.2. Greek

β	buffering capacity
ϵ	the highest acceptable pH variation
μ	mobility of the ion
σ	electrical conductivity

6.3. Subscripts

w	weak acid, water
s	strong acid
C	cathode
A	anode

6.4. Superscripts

0	refers to the initial time when the voltage was applied to the capillary
---	--

Acknowledgments

The author is grateful to Dr. N. Avdalovic for his support and improvements to the manuscript, Dr. J. Horvath for her help on the experimental part, Dr. R. Rocklin for his useful suggestions, and Ms. S. Morris for editorial assistance.

Appendix A

Electric conductivity of the solution is given by

$$\sigma = F([A_w]\mu_w K/(K + [H]) + [A_s]\mu_s + [B]\mu_B + [H]\mu_H + K_w/[H]\mu_{OH}) \quad (\text{A1})$$

where σ is the electric conductivity.

Ionic strength is given by

$$i = (1/2)([A_w]K/(K + [H]) + [A_s] + [B] + [H] + K_w/[H]) \quad (\text{A2})$$

where i is the ionic strength.

The equation for the evolution of the hydroxyl molarity in the cathode reservoir has the following form.

$$\begin{aligned} d[\text{OH}]/dt &= ([\text{H}]/[\text{OH}](1 + [A_w]K/(K + [H])^2) + 1) \\ &= (SE/V_A)([A_w]\mu_w K^2/(K + [H])^2 + [A_s]\mu_s \\ &\quad + \mu_B[B]), \end{aligned} \quad (\text{A3})$$

$$[\text{H}][\text{OH}] = K_w$$

References

- [1] H.E. Schwartz, M. Melera and R.G. Brownlee, *J. Chromatogr.*, 480 (1989) 129–139.
- [2] R.K. Iler, *The Chemistry of Silica*, 1979, Wiley, New York.
- [3] K.D. Lukacs and J.W. Jorgenson, *J. High Resolut. Chromatogr.*, 8 (1985) 407–411.
- [4] C. Schwer and E. Kennler, *Anal. Chem.*, 63 (1991) 1801–1807.
- [5] J.K. Towns and F.E. Regnier, *Anal. Chem.*, 63 (1991) 1126–1132.
- [6] W. Nashabeh and Z.E. Rassi, *J. Chromatogr.*, 559 (1991) 367–383.
- [7] J. Kohr and H. Engelhardt, *J. Chromatogr. A*, 652 (1993) 309–316.
- [8] M.S. Bello, L. Capelli and P.G. Righetti, *J. Chromatogr. A*, 684 (1994) 311–322.
- [9] M.A. Strega and A.L. Lagu, *J. Liquid Chromatogr.*, 16 (1993) 51–68.
- [10] H. Corstjens, H.A.H. Billet, J. Frank and K.C.A.M. Luyben, *Electrophoresis*, 17 (1996) 137–143.
- [11] A. Guttman and H.E. Schwartz, *Anal. Chem.*, 67 (1995) 2279–2283.